Molecular Crystals and Liquid Crystals
Publication details, including instructions for authors and subscription information:
http://www.tandfonline.com/loi/gmcl20

Study of Optical and Electrical Properties in Nematic Phase of Self Assembly Systems

N. Pongali Sathya Prabu [a], V. N. Vijayakumar [a] & M. L. N. Madhu Mohan [a]

[a] Liquid Crystal Research Laboratory (LCRL), Bannari Amman Institute of Technology, Sathyamangalam, 638 401, India

Version of record first published: 07 Oct 2011

To cite this article: N. Pongali Sathya Prabu, V. N. Vijayakumar & M. L. N. Madhu Mohan (2011): Study of Optical and Electrical Properties in Nematic Phase of Self Assembly Systems, Molecular Crystals and Liquid Crystals, 548:1, 73-85

To link to this article: http://dx.doi.org/10.1080/15421406.2011.590365

Mol. Cryst. Liq. Cryst., Vol. 548: pp. 73–85, 2011

ISSN: 1542-1406 print/1563-5287 online
DOI: 10.1080/15421406.2011.590365

Taylor & Francis
Taylor & Francis Group

Study of Optical and Electrical Properties in Nematic Phase of Self Assembly Systems

N. PONGALI SATHYA PRABU, V. N. VIJAYAKUMAR, AND M. L. N. MADHU MOHAN*

Liquid Crystal Research Laboratory (LCRL), Bannari Amman Institute of Technology, Sathyamangalam 638 401, India

Self assembly systems formed by hydroquinone (HQ) and alkyloxy benzoic acids (OBA) are isolated. HQ formed double hydrogen bonds with p-n-alkyloxy benzoic acids (nOBA). Various hydrogen-bonded complexes have been synthesized with HQ and decyloxy to dodecyloxy benzoic acid respectively. Fourier transform infrared spectra (FTIR) studies confirm the hydrogen bond formation in the complex. Polarizing optical microscopic (POM) studies revealed the textural information while the transition and enthalpy values are experimentally deduced from Differential scanning calorimetry (DSC) studies. Phase diagram has been constructed from the POM and DSC data respectively. Light modulation was observed in three hydrogen-bonded complexes and is studied by light intensity, helicoidal, textural, and dielectric studies.

Keywords Helix; hydroquinone; light modulation; nematic; p-n-alkyloxy benzoic acid

1. Introduction

Synthesis and characterization of self-assembly systems in liquid crystals referred as hydrogen-bonding liquid crystals gained importance and paved way for new type of soft materials. Kato and his research group [1–17] investigated many such systems with complementary components. The self assembly systems formed by alkyloxy carboxylic acids exhibits rich phase polymorphism. It has been previously reported by us that these self-organized systems induce variety of new phenomena, like reentrant phase occurrence [18,19], light modulation [20], optical-shuttering action [21–24], and field induced transitions [20,25,26].

The carboxylic acids with other acids are reported [18–26] to form complementary single and multiple hydrogen bonds. We have already reported [19] the ambient Smectic ordering observed in the hydrogen bonded complex formed between carboxylic acids and anilines that individually exhibits mesogenic properties and in turn, the H-bonds has pronounced effect in bringing down the phase transition temperature. However, there are reports in the literature [27,28] to obtain a mesogenic hydrogen-bonded liquid crystals (HBLC), it is enough if one of the compounds exhibits mesogenic properties. It is a great surprise to note that a mesogenic HBLC can be formed through two nonmesogenic compounds [29–30] by hydrogen bonding. Thus, it can be inferred that depending upon

*Address correspondence to M. L. N. Madhu Mohan, Liquid Crystal Research Laboratory (LCRL), Bannari Amman Institute of Technology, Sathyamangalam 638 401, India. E-mail: mln.madhu@gmail.com

the position of the hydrogen bonding and chemical structure of the individual compounds, hydrogen bonding can induce liquid crystallinity and also plays a pivotal role in bringing down considerably the magnitude of the phase transition temperatures.

In the present work, a successful attempt has been made to design and isolate a homologous series of HBLC. The mesogenic p-n-alkyloxy benzoic acids (nOBA) (where, n represents the alkyloxy carbon number from 5 to 12) formed a HBLC with hydroquinone (HQ) respectively. Phase diagrams, mesogenic phase, and thermal range are discussed. Light modulation action is characterized by optical textural, light intensity, and dielectric studies.

2. Experimental

Optical textural observations were made with a Nikon polarizing microscope equipped with Nikon digital charge-coupled devices (CCD) camera system with 5 mega pixels and 2560 × 1920 pixel resolutions. The liquid crystalline textures were processed, analyzed, and stored with the aid of ACT-2U imaging software system. The temperature control of the liquid crystal cell was equipped by Instec HCS402-STC 200 temperature controller (Instec, USA) to a temperature resolution of ±0.1°C. This unit is interfaced to computer by IEEE –STC 200 to control and monitor the temperature. The liquid crystal sample is filled by capillary action in its isotropic state into a commercially available (Instec, USA) polyamide buffed cell with 5 micron spacer. The transition temperatures and corresponding enthalpy values were obtained by DSC (Shimadzu DSC-60, Japan). Fourier transform infrared spectra (FTIR) spectra was recorded (ABB FTIR MB3000) and analyzed with the MB3000 software. Dielectric studies were performed using impedance analyzer (Agilent LF 4192A, USA). The nOBA and HQ were supplied by Sigma Aldrich, Germany and all the solvents used were HPLC grade.

2.1 Synthesis of HBLC

Intermolecular hydrogen bonded mesogens are synthesized by the addition of two moles of (nOBA) with one mole of HQ in N,N-Dimethyl formamide (DMF) respectively. Further they are subject to constant stirring for 14 hours at ambient temperature of 30°C till a white precipitate in a dense solution is formed. The white crystalline crude complexes so obtained by removing excess DMF are then recrystallized with dimethyl Sulfoxide (DMSO) and the yield varied from 85% to 95%. Yield of higher homologues complexes are observed to be more compared to its lower counterparts. The molecular structure of the present homologous series of nOBA with HQ is depicted in the Fig. 1, where n represents the alkyloxy carbon number. From Fig. 1, the alternate hydrogen bonded sites situated on either sides of benzene ring moiety of the HQ can be identified.

3. Results and Discussion

All the hydrogen-bonded complexes isolated under the present investigation mostly are white crystalline solids and are stable at room temperature. They are insoluble in water and sparingly soluble in common organic solvents, such as methanol, ethanol, benzene, and

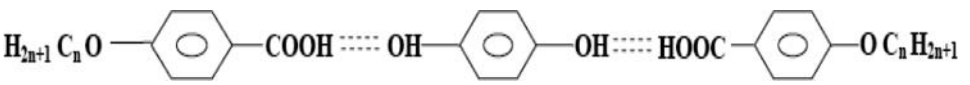

Figure 1. Molecular structure of HQ + nOBA series.

dichloro methane. However, they show a high degree of solubility in coordinating solvents, like DMSO, DMF, and pyridine. All these mesogens melt at specific temperatures below 141°C. They show high thermal and chemical stability when subjected to repeated thermal scans performed during POM and DSC studies.

3.1 Phase Identification

The observed phase variants, transition temperatures and corresponding enthalpy values obtained by DSC in cooling and heating cycles for the HQ + nOBA complexes are presented in Table 1.

3.2 HQ + nOBA Homologous Series

The mesogens of the HQ and alkyloxy benzoic acid (OBA) homologous series are found to exhibit characteristic textures [31], viz., Nematic (schlieren texture), Smectic C (broken focal conic texture), Smectic F (chequered board texture), and Smectic G (multi colored smooth mosaic texture), respectively. The general phase sequence of the HQ and OBA in the cooling run can be shown as:

Isotropic → Nematic → Sm F → Crystal	(HQ + 5OBA), (HQ + 6OBA)
Isotropic → Nematic → Sm C → Sm F → Crystal	(HQ + 7OBA), (HQ + 8OBA), (HQ + 9OBA)
Isotropic → Nematic → Sm C → Sm G → Crystal	(HQ + 10OBA), (HQ + 11OBA), (HQ + 12OBA)

Table 1. Transition temperatures and enthalpy values obtained by various techniques

Complex	Phase variance	Study	Crystal to melt	N	C	G	Crystal
HQ + 10OBA	NCG	DSC[c]	87.1 (65.01)	132.8 (12.36)	119.1 (3.76)	97.2 (34.41)	
		DSC[b]		128.4 (13.48)	115.3 (4.11)	91.5 (24.05)	73.8 (32.80)
		POM[b]		128.9	119.7	92.9	74.2
HQ + 11OBA	NCG	DSC[c]	97.3 (93.56)	132.3 (8.65)	125.8 (4.66)	[a]	
		DSC[b]		128.2 (7.04)	121.7 (4.47)	84.9 (24.02)	78.0 (61.76)
		POM[b]		128.8	122.4	85.3	78.7
HQ + 12OBA	NCG	DSC[c]	96.3 (97.89)	[a]	[a]	[a]	
		DSC[b]		130.1 (7.84)	124.8 (8.01)	119.9 (17.87)	86.7 (27.76)
		POM[b]		130.8	125.4	120.4	87.5

[a]No phase observed.
[b]Cooling run.
[c]Heating run.

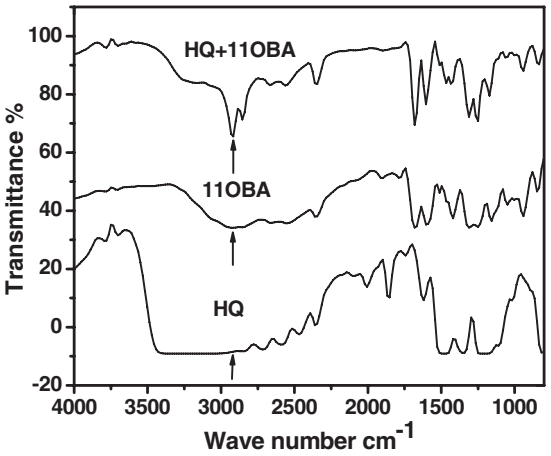

Figure 2. FTIR spectra of HQ, 11OBA and HQ + 11OBA complex.

3.3 Infrared (IR) Spectroscopy

IR spectra of free nOBA, HQ, and their intermolecular hydrogen-bonded complexes are recorded in the solid state (KBr) at room temperature. Figure 2 illustrates the FTIR spectra of HQ, dodecyloxy benzoic acid (11OBA), and the corresponding hydrogen-bonded complex (HQ + 11OBA) in solid state at room temperature as a representative case. A noteworthy feature in the spectra of HQ + 11OBA complex is the appearance of the sharp high intense band at 2916 cm^{-1} and nonappearance of the same in HQ and 11OBA compounds, which clearly suggests the formation of hydrogen bond upon complexation. Further, the related literature [28,32,33] strongly conform the formation of hydrogen bond and its existence in the monomeric form upon complexation.

3.4 DSC Studies

DSC thermograms are obtained in heating and cooling cycle. The sample is heated with a scan rate of 10°C/min and hold at its isotropic temperature for 2 min. so as to attain thermal stability. The cooling run is performed with a scan rate of 10°C/min. The respective equilibrium transition temperatures and corresponding enthalpy values of the mesogens of the homologous series are listed separately in Table 1. Polarizing optical microscopic studies also confirm these DSC transition temperatures.

3.4.1 DSC Studies of HQ + 10OBA. The phase transition temperatures and enthalpy values of decyloxy benzoic acid and HQ mesogen (HQ + 10OBA) are discussed as a representative case. The DSC thermogram of HQ + 10OBA is illustrated in Fig. 3. From which, it can be inferred that in the DSC heating run exhibits four exothermic peaks at 87.1°C, 97.2°C, 119.1°C, and 132.8°C with enthalpy values of 65.01 J/g, 34.41 J/g, 3.76 J/g, and 12.36 J/g, respectively. These four peaks correspond to the crystal to melt to Smectic G to Smectic C and Smectic C to Nematic phase transitions. In the cooling run this sample exhibits four peaks at 128.4°C, 115.3°C, 91.5°C, and 73.8°C with enthalpy values of 13.48 J/g, 4.11 J/g, 24.05 J/g, and 32.80 J/g, respectively. These endothermic peaks correspond to the isotropic to Nematic, Nematic to Smectic C, Smectic C to Smectic G, and Smectic G to crystal phases, respectively.

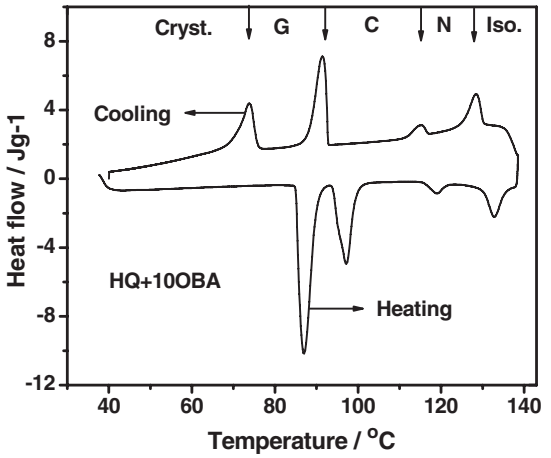

Figure 3. DSC thermogram of HQ + 10OBA complex.

3.5 Phase Diagram of Pure p-n-Alkyloxy Benzoic Acids

The phase diagram of pure nOBA is reported [34] while the HQ + nOBA homologous series is constructed through optical polarizing microscopic studies and by the phase transition temperatures observed in the cooling run of the DSC thermogram. The phase diagram of pure nOBA is reported [28,34] to compose of two phases, namely Nematic and Smectic C.

3.5.1 Phase Diagram of HQ + nOBA. The phase diagram of HQ and OBA is depicted in Fig. 4. The following points can be elucidated from Fig. 4:

(1) The HQ + nOBA hydrogen bonded homologous series exhibits orthogonal and titled phases; namely Nematic and Smectic C, Smectic F, Smectic G phases, respectively.
(2) The total thermal range of the mesogenic phases increased with increase in the alkyloxy carbon number up to octyloxy carbon and then starts to decrease till dodecyloxy benzoic acid.

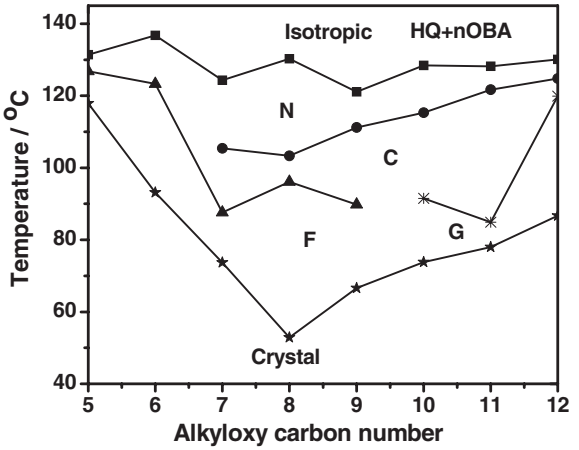

Figure 4. Phase diagram of HQ + nOBA series.

(3) Nematic phase is observed in all the complexes of the present homologous series.
(4) The Smectic C phase is induced in the higher homologous members from heptyloxy benzoic acid and continued till dodecyloxy carbon. The thermal phase width is largest for undecyloxy carbon and narrowest for dodecyloxy carbon.
(5) A higher ordered phase Smectic G phase is observed in HQ + 10OBA complex quenching Smectic F phase thermal range.
(6) A systematic decrease in the crystallization temperatures is observed up to octyloxy benzoic carbon number up on which the crystallization temperatures starts to increase proportionally along with its corresponding carbon number.
(7) One of the interesting observations in the present series is the detection of odd–even effect at isotropic to Nematic phase transition with respect to enthalpy values and the corresponding transition temperatures.

4. Light Modulation

Three hydrogen complexes HQ + 10OBA, HQ + 11OBA, and HQ + 12OBA in Nematic phase, when subjected to an external bias field exhibited light modulation. It is worth mentioning that when the external bias field is withdrawn, the original Nematic texture is instantaneously retained, thus, this light modulation action is reversible. Furthermore, this light modulation is noticed in the entire Nematic thermal span of the respective complex.

The light modulation is characterized by helicoidal structural, optical textural, dielectric, and light intensity studies. The complexes are filled in different five micron homogenously aligned parallel cells of 5 mm × 5 mm active area (Instec, USA). Silver wires as leads are drawn from the cell for electrical connections. The cell is placed in the hot and cold stage (Instec) and observed under crossed polarizer's of polarizing microscope.

4.1 Electrical and Elastic Torques

The deformation of Nematic liquid crystal with the applied external stimulus at the boundaries plays an important role to orient thin samples of low magnitude of helix. The molecules are uniformly aligned at the substrates by boundary interactions. This homeotropic interaction is characterized by orientation of the director perpendicular to the bounding walls. The orientation of the Nematic liquid crystal between two substrates depends on the relative magnitude of the deforming electric torque and the restoring elastic torque of the Nematic liquid crystal. It is reported [35] that the field induced deformations occur because of the destabilizing electric torque, which overcomes the stabilizing elastic torque.

The various threshold voltage values corresponding to HQ + 10OBA, HQ + 11OBA, and HQ + 12OBA complexes are given in Table 2. The decrease in the magnitude of the threshold values can be justified by correlating it with the anchoring energy. As the anchoring energy is decreased with increase in the alkyloxy carbon number, thus, the threshold values are decreased as can be noticed from Table 2.

Table 2. Optical, thermal, and electrical data of HQ + nOBA complexes

Complex	Nematic thermal range (°C)	Threshold field value (V/μ)	Field transitions	Percentage of light modulation
HQ + 10OBA	13.1	3.5	$E_0 \rightarrow E_1$	79
HQ + 11OBA	6.5	1.4	$E_0 \rightarrow E_1$	51
HQ + 12OBA	5.3	2.0	$E_0 \rightarrow E_1$	63

The following sections discuss the light modulation action studied by various techniques.

4.2 Textural Observations

The respective complex under investigation is taken to isotropic state and cooled at a programmed mode to a desired temperature to obtain Nematic phase (Plates 1, 3, and 5). The external stimulus from impedance analyzer is slowly increased in small steps of 0.5 volts/micron and the texture of the phase is recorded. As a representative case, in HQ + 10OBA complex as the voltage reaches a value of 3.5 volts/micron the mesogen behaves like an optical modulator in the sense that the schlieren texture of Nematic disappears and optical extinction is observed (Plate 2). Similarly, the hydrogen bonded complexes of HQ + 11OBA and HQ + 12OBA in the Nematic phase exhibited optical modulation (Plates 4 and 6) when the field reached values of 1.4 and 2.0 respectively. Odd complex (HQ + 11OBA) has the lowest threshold value compared the even complexes (HQ + 10OBA, HQ + 12OBA). Steric hindrance of the OBA plays a vital role in determining the threshold values.

Table 2 gives the values of the various voltages for the three hydrogen-bonded complexes. These voltages are referred to as threshold voltage. Voltage below the threshold values is referred to as E_0 state while any voltage greater than or equal to threshold voltage enables the light modulation action, and is designated as E_1. This phase is referred to as an optical modulator. The phase transitions for all the three complexes can be given as:

$$E_0 \text{ (Schlieren texture)} \rightarrow E_1 \text{ (Optical modulator)}$$

4.3 Optical Intensity Studies

The optical intensity in the Nematic phase exhibited by the complexes under the influence of the external stimulus at a constant temperature is studied. A photo diode (TSL 252) is used to measure the optical intensity tracked at the eye piece of the polarizing microscope and the corresponding voltage is measured with the aid of a 61/2 Keithley multi meter (2100).

Figures 5–7 illustrate the light intensity profile with applied external field. In all the complexes, at the respective threshold value, the light intensity steeply falls indicating the onset of E_1 phase, which is referred to as light modulation action. The alignment of the molecules with the external stimulus and the anchoring energy of the molecules to the glass substrate of the liquid crystal cell containing the respective complexes are responsible for the above behavior. The percentage of the light inhibited at the threshold value is tabulated in Table 2.

4.4 Dielectric Analysis

The permittivity data obtained at various voltages of different polarities for HQ + 10OBA, HQ + 11OBA, and HQ + 12OBA are plotted in Figs. 8–10 respectively. Following points can be observed from the Figs. 8–10:

(1) A symmetrical decrement of the permittivity is observed in both the polarities indicating a unique dipolar reorientation process that is independent of the polarity of the external stimulus.
(2) A linear decrement of the permittivity value is noticed in both polarities till the threshold value (E_1) of the field. The molecular realignment is one of the reasons for the steep decrease in the permittivity value.

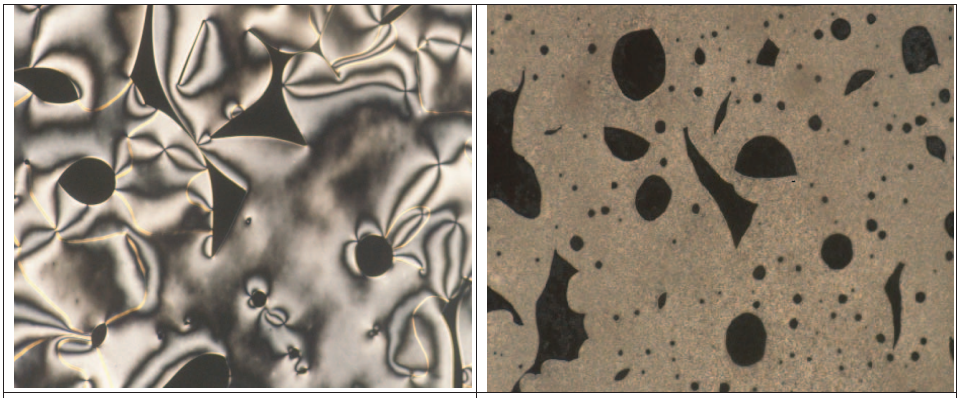

Plate 1

Plate 2

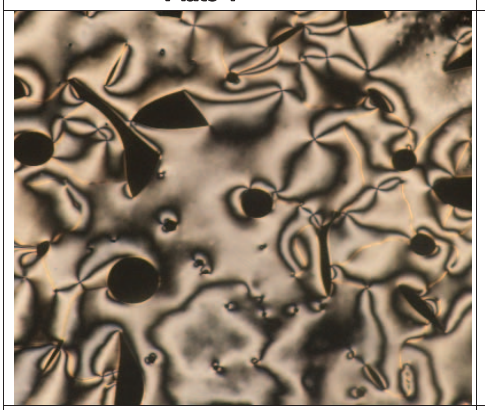

Plate 3

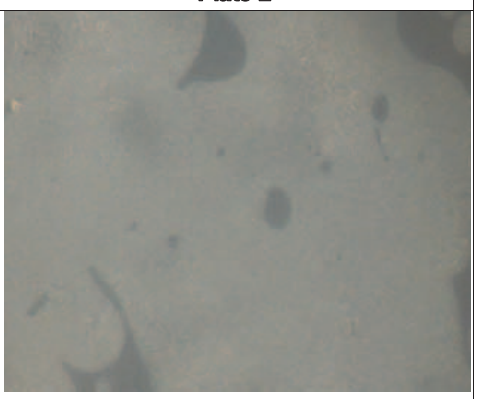

Plate 4

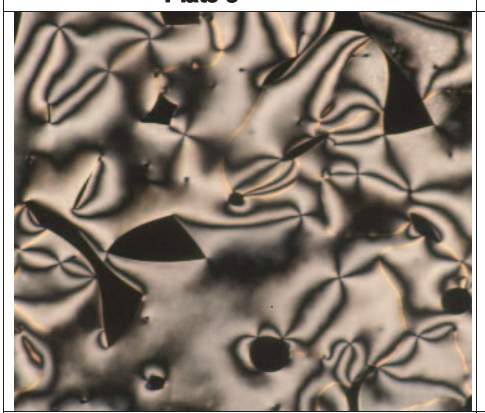

Plate 5

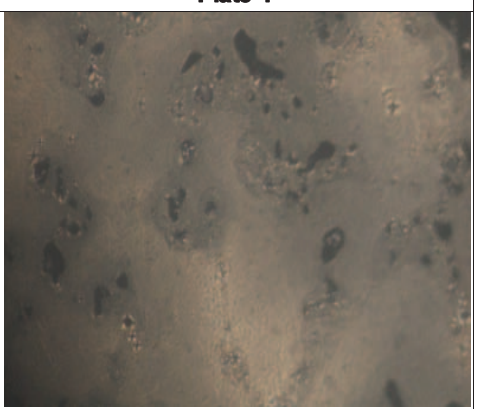

Plate 6

Plates . (1) Nematic schlieren texture of HQ + 10OBA complex at E_0 transition; (2) Field deformed texture of HQ + 10OBA complex at E_1 transition; (3) Nematic schlieren texture of HQ + 11OBA complex at E_0 transition; (4) Field deformed texture of HQ + 11OBA complex at E_1 transition; (5) Nematic schlieren texture of HQ + 12OBA complex at E_0 transition; (6) Field deformed texture of HQ + 12OBA complex at E_1 transition.

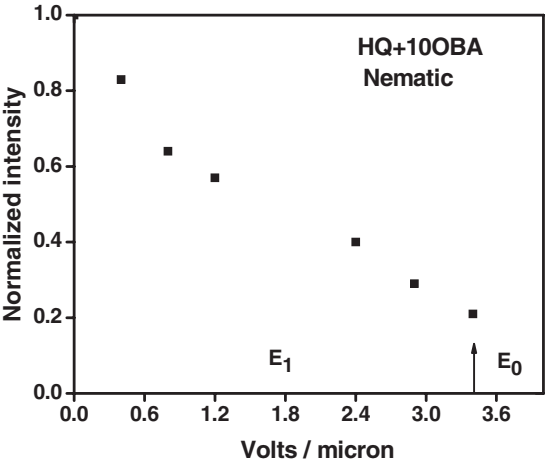

Figure 5. Variation of light intensity with applied stimulus for HQ + 10OBA complex.

(3) At the threshold value (E_1), the permittivity values in both polarities saturate indicating the onset of the light modulation process.

4.5 Deformation of Helicoidal Structure with Applied Field

In the literature, it is reported [36–42] that the distortion and unwinding of the helicoidal structure with applied field in the liquid crystal mesogen yield field induced deformations. The untwisting of the helical structure of a HBLC in a thin plane layer exposed to an external action (temperature or field) and its dependence on the molecular adhesive forces at the layer boundaries are studied.

In the present work, the helical pitch is measured by diffraction of He-Ne red laser light on liquid crystal sample filled in a commercial available (Instec) buffed conducting cell. This method can be used to measure the helical pitch of short length.

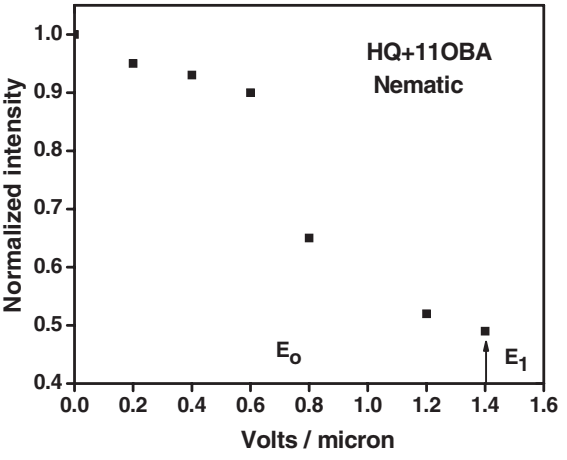

Figure 6. Variation of light intensity with applied stimulus for HQ + 11OBA complex.

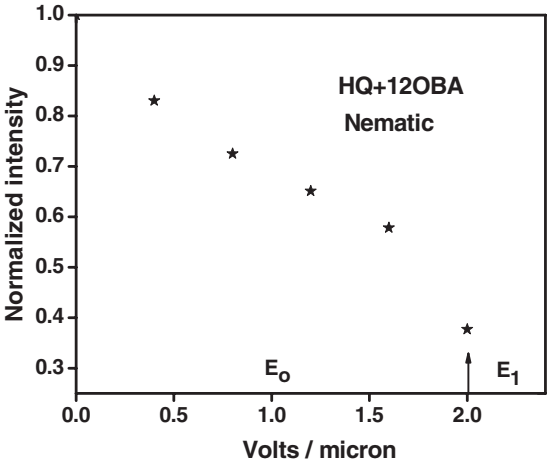

Figure 7. Variation of light intensity with applied stimulus for HQ + 12OBA complex.

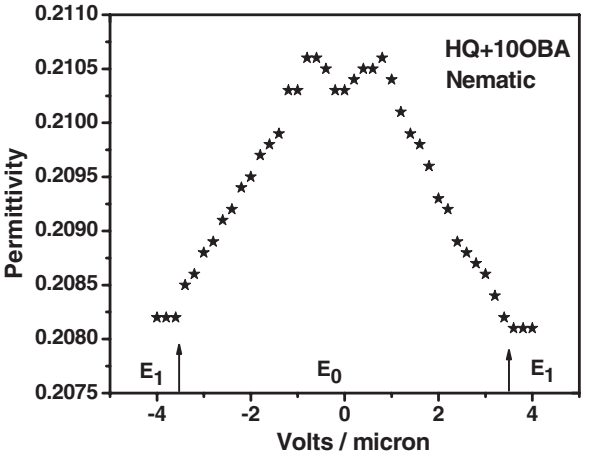

Figure 8. Variation of permittivity with applied stimulus for HQ + 10OBA complex.

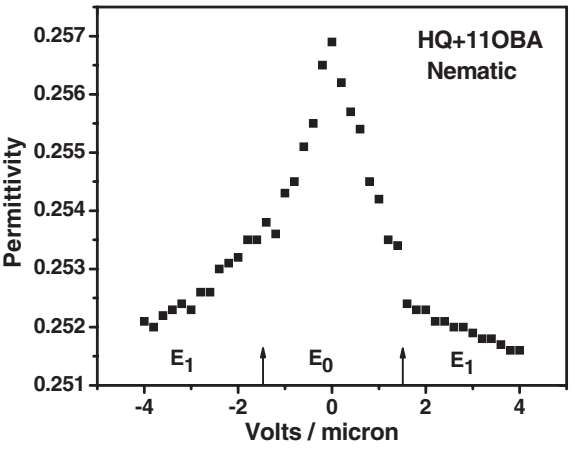

Figure 9. Variation of permittivity with applied stimulus for HQ + 11OBA complex.

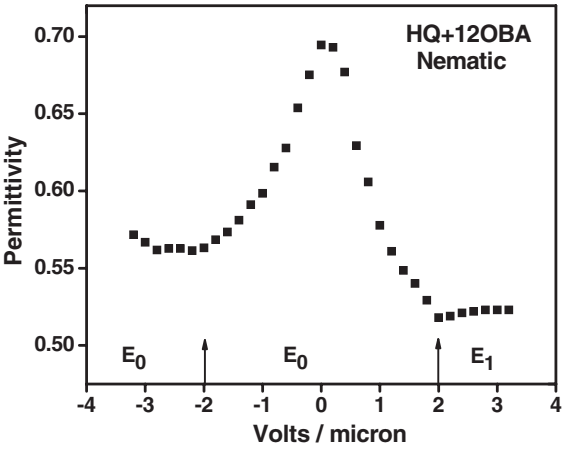

Figure 10. Variation of permittivity with applied stimulus for HQ + 12OBA complex.

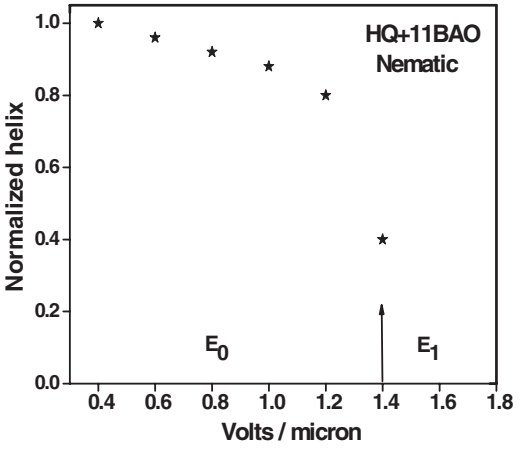

Figure 11. Variation of HELIX with applied stimulus for HQ + 10OBA complex.

The present compound of HQ + 11OBA is filled in such a commercially available cell and silver leads are drawn for contact. The deformation of the helicoidal structure has been experimentally analyzed by applying external electrical stimulus drawn from impedance analyzer. The variation of the helix is noted at each step of the applied stimulus. The decrement of the magnitude of helix of HQ + 11OBA manifesting the distortion of the helix is shown in Fig. 11. It is pertinent to mention that the intensity of the light profile from the liquid crystal cell under crossed polarizer gradually decreased (Fig. 11 and Plate 4) At the threshold voltage values (E_1) discussed in the above section, the helix completely unwound in turn the light extinction is observed. Hence, these HBLC materials may be used as a light modulator.

Similar trends of results are observed in HQ + 10OBA and HQ + 12OBA of the present homologous series.

Acknowledgments

One of the authors (M. L. N. Madhu Mohan) acknowledges the financial support rendered by All India Council for Technical Education (AICTE), Department of Science and Technology (DST), and Defense Research Development Organization (DRDO), New Delhi. Infrastructural support provided by Bannari Amman Institute of Technology is gratefully acknowledged.

References

[1] Kihara, H., Kato, T., Uryu, T., and Frechet, J. M. J. (1996). *Chem. Mater.*, **8**, 961.
[2] Kato, T. and Frechet, J. M. J. (1995). *Macromol. Symp.*, **98**, 311.
[3] Kato, T. and Frechet, J. M. J. (1989). *J. Am. Chem. Soc.*, **111**, 8533.
[4] Kato, T. and Frechet, J. M. J. (1989). *Macromolecules.*, **22**, 3818.
[5] Kato, T., Nakano, M., Moteki, T., Uryu, T., and Ujiie, S. (1995). *Macromolecules.*, **28**, 8875.
[6] Kato, T., Frechet, J. M. J., Wilson, P. G., Saito, T., Uryu, T., Fujishima, A., Jin, C., and Kaneuchi, F. (1993). *Chem. Mater.*, **5**, 1094.
[7] Kato, T., Wilson, P. G., Fujishima, A., and Frechet, J. M. J. (1990). *Chem. Lett.*, **19**(11), 2003.
[8] Kato, T., Fukumasa, M., and Frechet, J. M. J. (1995). *Chem. Mater.*, **7**, 368.
[9] Fukumasa, M., Kato, T., Uryu, T., Frechet, J. M. J. (1993) *Chem. Lett.*, **22**(1), 65.
[10] Kato, T., Fujishima, A., and Frechet, J. M. J. (1990). *Chem. Lett.*, **19**(6), 919.
[11] Kato, T., Adachi, H., Fujishima, A., and Frechet, J. M. J. (1992). *Chem. Lett.*, **21**(2), 265.
[12] Kato, T., Uryu, T., Kaneuchi, F., Jin, C., and Frechet, J. M. J. (1993). *Liq. Cryst.*, **14**, 1311.
[13] Kato, T., Kihara, H., Uryu, T., Ujiie, S., Limura, K., Frechet, J. M. J., and Kumar, U. (1993). *Ferroelectrics.*, **148**, 161.
[14] Kumar, U., Frechet, J. M. J., Kato, T., Ujiie, S., and Limura, K. (1992). *Angew. Chem., Int. Ed. Engl.*, **31**, 1531.
[15] Kumar, U., Kato, T., and Frechet, J. M. J. (1992). *J. Am. Chem. Soc.*, **114**, 6630.
[16] Kato, T., Kihara, H., Uryu, T., Fujishima, A., and Frechet, J. M. J. (1992). *Macromolecules.*, **25**, 6836.
[17] Kato, T., Kihara, H., Kumar, U., Uryu, T., and Frechet, J. M. J. (1994). *Angew. Chem., Int, Ed. Engl.*, **33**, 1644.
[18] Vijayakumar, V. N., Mugugadass, K., and Madhu Mohan, M. L. N. (2010). *Mol. Cryst. Liq. Cryst.*, **517**, 41.
[19] Chitravel, T. and Madhu Mohan, M. L. N. (2010). *Mol. Cryst. Liq. Cryst.*, **524**, 131.
[20] Vijayakumar, V. N. and Madhu Mohan, M. L. N. (2010). *Mol. Cryst. Liq. Cryst.*, **517**, 113.
[21] Vijayakumar, V. N. and Madhu Mohan, M. L. N. (2009). *J. Opto. Elec. Adv. Mat.*, **11**(8), 1139.
[22] Vijayakumar, V. N. and Madhu Mohan, M. L. N. (2010). *Mol. Cryst. Liq. Cryst.*, **524**, 54.
[23] Vijayakumar, V. N. and Madhu Mohan, M. L. N. (2009). *Sol. State. Sci.*, **4**, 482.
[24] Vijayakumar, V. N. and Madhu Mohan, M. L. N. (2009). *Braz J..Phy.*, **39**(4), 677.
[25] Vijayakumar, V. N. and Madhu Mohan, M. L. N. (2011). *Optik-Int. J. Light Electron Opt.*, (in press, doi: 10.1016/j.ijleo.2011.07.028).
[26] Vijayakumar, V. N. and Madhu Mohan, M. L. N. (2009). *Sol. State. Comm.*, **149**, 2090.
[27] Tian, Y. Q., He, X., Zhao, Y. Y., Tang, X. Y., Jin Li, T., and Huang, X. M. (1998). *Mol. Cryst. Liq. Cryst.*, **309**, 19.
[28] Swathi, P., Kumar, P. A., Pisipati, V. G. K. M., Rajeshwari, A. V., Sreehari Sastry, S., and Murthy, P. N. (2002). *Z. Natur Forsch*, **57a**, 797.
[29] Hentrich, F., Diele, S. and Tschierske, C. (1994). *Liq. Cryst.*, **17**, 827.
[30] Kobayashi, Y. and Matsunage, Y. (1987). *Bull. Chem. Soc. Jpn.*, **60**, 3515.
[31] Gray, G. W. and Goodby, J. W. G. (1984). *Smectic Liquid Crystals: Textures and Structures*, Leonard Hill: London.
[32] Nakamoto, K. (1978). *Infrared and Raman Spectra of Inorganic and Co-ordination Compounds*, Interscience: New York.

[33] Cook, A. G., Baumeister, U., and Tschierske, C. (2005). *J. Mater. Chem.*, **15**, 1708.
[34] Srinivasulu, M., Satyanarayana, P. V. V., Kumar, P. A., and Pisipati, V. G. K. M. (2002). *Z. Naturforsch., A: Phys. Sci.*, **56a**, 685.
[35] Stegemeyer, H. (Ed.). (1994). *Liquid Crystals*, Springer: New York.
[36] Petit, M., Daoudi, A., Ismaili, M., and Buisine, J. M. (2006). *Eur Phys J E Soft Matter.*, **20**, 327.
[37] Abdulhalim, I. and Moddel, G. (1991). *Mol. Cryst. Liq. Cryst.*, **200**, 79.
[38] Judge, L. A., Kriezis, E. E., and Elston, S. J. (2001). *Mol. Cryst. Liq. Cryst.*, **366**, 661.
[39] Schiller, P. and Zeitler, F. (1997). *Phys. Rev E 5*, **6**, 531.
[40] Schiller, P. and Zeitler, F. (1995). *J. de Physique II*, **5**, 1835.
[41] Zeldovich, B. Y. and Tabiryan, N. V. (1981). *JETP Lett.*, **34**, 406.
[42] Belyakov, V. A. (2002). *JETP Lett.*, **76**, 88.